

Discovery of 1,8-Disubstituted-[1,2,3]triazolo[4,5-c]quinoline Derivatives as a New Class of Hippo Signaling Pathway Inhibitors

Jingxin Qiao, Guifeng Lin, Anjie Xia, Zhiyu Xiang, Pei Chen, Guo Zhang, Linli Li, Shengyong Yang

PII: S0960-894X(19)30527-X
DOI: <https://doi.org/10.1016/j.bmcl.2019.08.001>
Reference: BMCL 26597

To appear in: *Bioorganic & Medicinal Chemistry Letters*

Received Date: 23 April 2019
Revised Date: 11 July 2019
Accepted Date: 1 August 2019

Please cite this article as: Qiao, J., Lin, G., Xia, A., Xiang, Z., Chen, P., Zhang, G., Li, L., Yang, S., Discovery of 1,8-Disubstituted-[1,2,3]triazolo[4,5-c]quinoline Derivatives as a New Class of Hippo Signaling Pathway Inhibitors, *Bioorganic & Medicinal Chemistry Letters* (2019), doi: <https://doi.org/10.1016/j.bmcl.2019.08.001>

This is a PDF file of an article that has undergone enhancements after acceptance, such as the addition of a cover page and metadata, and formatting for readability, but it is not yet the definitive version of record. This version will undergo additional copyediting, typesetting and review before it is published in its final form, but we are providing this version to give early visibility of the article. Please note that, during the production process, errors may be discovered which could affect the content, and all legal disclaimers that apply to the journal pertain.



**Discovery of 1,8-Disubstituted-[1,2,3]triazolo[4,5-c]quinoline Derivatives as a
New Class of Hippo Signaling Pathway Inhibitors**

Jingxin Qiao^{a,#}, Guifeng Lin^{a,#}, Anjie Xia^{a,#}, Zhiyu Xiang^a, Pei Chen^b, Guo Zhang^a,

Linli Li^b, Shengyong Yang^{a,*}

^a *State Key Laboratory of Biotherapy and Cancer Center, West China Hospital, Sichuan University, Chengdu, Sichuan 610041, China*

^b *Key Laboratory of Drug Targeting and Drug Delivery System of Ministry of Education, West China School of Pharmacy, Sichuan University, Sichuan 610041, China*

These authors contributed to this work equally

* Corresponding author. State Key Laboratory of Biotherapy and Cancer Center, West China Hospital, Sichuan University, Chengdu, Sichuan 610041, China. Tel.: +86-28-85164063; fax: +86-28-85164060. E-mail address: yangsy@scu.edu.cn

ABSTRACT

Inhibitors of the Hippo signaling pathway have been demonstrated to have a potential clinical application in cases such as tissue repair and organ regeneration. However, there is a lack of potent Hippo pathway inhibitors at present. Herein we report the discovery of a series of 1,8-disubstituted-[1,2,3]triazolo[4,5-*c*]quinoline derivatives as a new class of Hippo pathway inhibitors by utilizing a cell line-based screening model (A549-CTGF). Structure-activity relationship (SAR) of these compounds was also discussed. The most potent compound in the A549-CTGF cell assay, **11g**, was then evaluated by real-time PCR and immunofluorescence assays. Overall, this study provides a starting point for later drug discovery targeting the Hippo signaling pathway.

Keywords

Hippo signaling pathway, tissue repair and organ regeneration, small molecule inhibitor, structure-activity relationship

The Hippo pathway is an evolutionarily conserved signaling module that plays critical roles in organ size control, tissue repair, and organ regeneration, as well as tumorigenesis.¹⁻⁵ Core components of the Hippo pathway include the mammalian Ste20-like kinases (Mst1/2), the cofactor Salvador (Sav1), the large tumor suppressor (Lats1/2), and two downstream effectors Yes-associated protein (YAP) and the transcriptional co-activator with PDZ-binding motif (TAZ).⁶⁻⁸ It has been established that Mst1/2 and Sav1 form a complex to phosphorylate and activate Lats1/2, and Lats1/2 kinases in turn phosphorylate and inhibit the transcription co-activators, YAP and TAZ.^{9,10} Numerous studies have shown that inactivation of the Hippo pathway could lead YAP/TAZ (un-phosphorylated) to translocate into the nucleus and promote transcription of pro-proliferative and pro-survival genes,⁹⁻¹² hence benefiting the tissue repair and organ regeneration,¹³⁻¹⁹ which implies a potential clinical application of small molecule inhibitors of Hippo pathway. Discovery of small molecule inhibitors of the Hippo pathway has thus attracted much attention in recent years.^{1,3,4,15}

Despite great efforts, small molecule inhibitors of the Hippo pathway are still rare. Currently, only one compound, 4-((5,10-dimethyl-6-oxo-6,10-dihydro- 5*H*-pyrimido[5,4-*b*]thieno[3,2-*e*][1,4]diazepin-2-yl)amino)benzenesulfonamide (**XMU-MP-1**), has been reported to be able to efficiently inhibit the Hippo pathway and displayed ability to promote the repair and regeneration of damaged liver and intestinal.¹ To discover more new potent Hippo pathway inhibitors, we in this investigation established a cell line-based screening model in advance, which is an A549 cell line that stably expresses firefly luciferase driven by connective tissue growth factor (CTGF) promoter and Renilla luciferase driven by cytomegalovirus (CMV) promoter (called A549-CTGF cells hereafter); CTGF is a target gene of Hippo pathway.²⁰ As expected, **XMU-MP-1** treatment increased the relative level of firefly

luciferase in a concentration-dependent manner (Figure 1A). To further confirm the up-regulation of CTGF expression induced by **XMU-MP-1**, mRNA level of endogenous CTGF in A549-CTGF cells was detected by real-time PCR. Consistent with the dual-luciferase reporter assays, the mRNA level of endogenous CTGF was up-regulated by **XMU-MP-1** treatment (Figure 1B). These results demonstrated the effectiveness of the A549-CTGF screening model. We then used this model to screen our own chemical library containing about 2000 unique compounds synthesized by our group, which results are shown in Figure 1C. A number of compounds were found to be able to inhibit the Hippo pathway. The most potent one corresponds to compound (*S*)-1-(1-(3-fluorophenyl)ethyl)-8-(1*H*-pyrrolo[2,3-*b*]pyridin-5-yl)-2,3-dihydro-1*H*-[1,2,3]triazolo[4,5-*c*]quinoline (**T111**), which showed similar activity with **XMU-MP-1** in this assay. **T111** was then chosen as a hit compound for further structural optimization.

The structural optimization was focused on two regions of **T111** (**R**¹, **R**²; Figure 2). Various substituents were used to replace **R**¹ and **R**², and a total of 28 new compounds were synthesized. Bioactivities of these compounds were measured by the A549-CTGF cell assay.

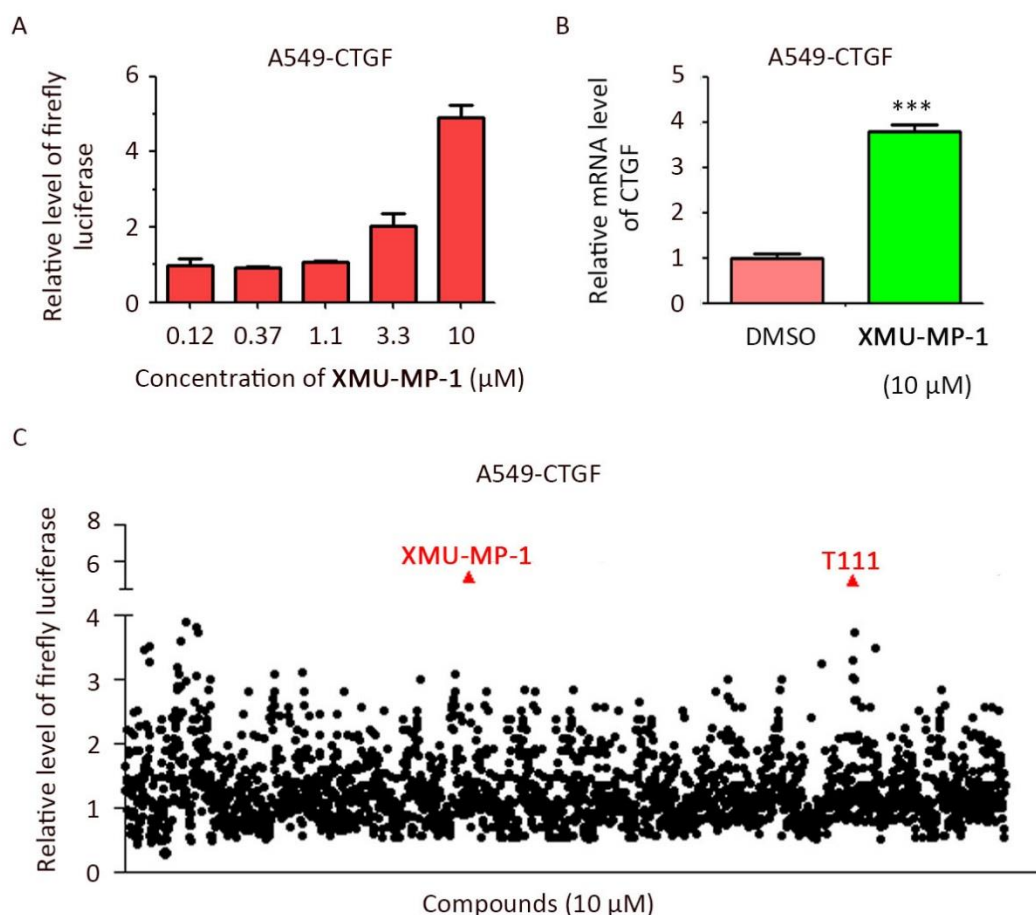


Figure 1. (A) **XMU-MP-1** effectively increased relative firefly luciferase level of the A549-CTGF cells in a concentration-dependent manner. Dual-luciferase reporter assays of A549-CTGF cells were performed after 24 h culture in the presence of **XMU-MP-1**. Data are represented as mean \pm SEM of three independent experiments. The relative firefly luciferase level of dimethyl sulfoxide (DMSO)-treated A549-CTGF cells was arbitrarily taken as 1. (B) **XMU-MP-1** was able to up-regulate endogenous CTGF mRNA levels in A549-CTGF cells. A549-CTGF cells were treated with **XMU-MP-1** (10 μ M) or DMSO (0.1%) for 24 h, and total RNA was extracted. The mRNA level of endogenous CTGF in A549-CTGF cells was detected by real-time PCR. (C) Screening results of about 2,000 compounds at the concentration of 10 μ M by the dual-luciferase reporter assays. The relative firefly luciferase level of DMSO-treated A549-

CTGF cells was arbitrarily taken as 1.

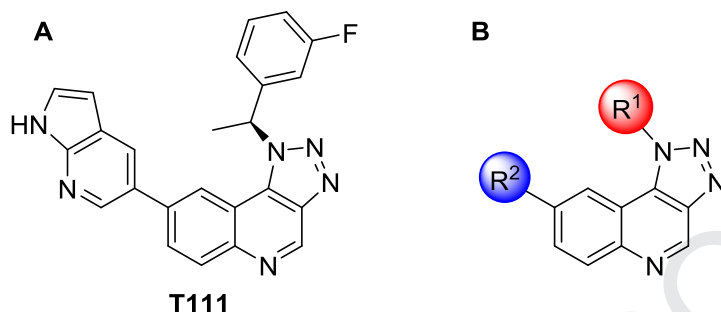
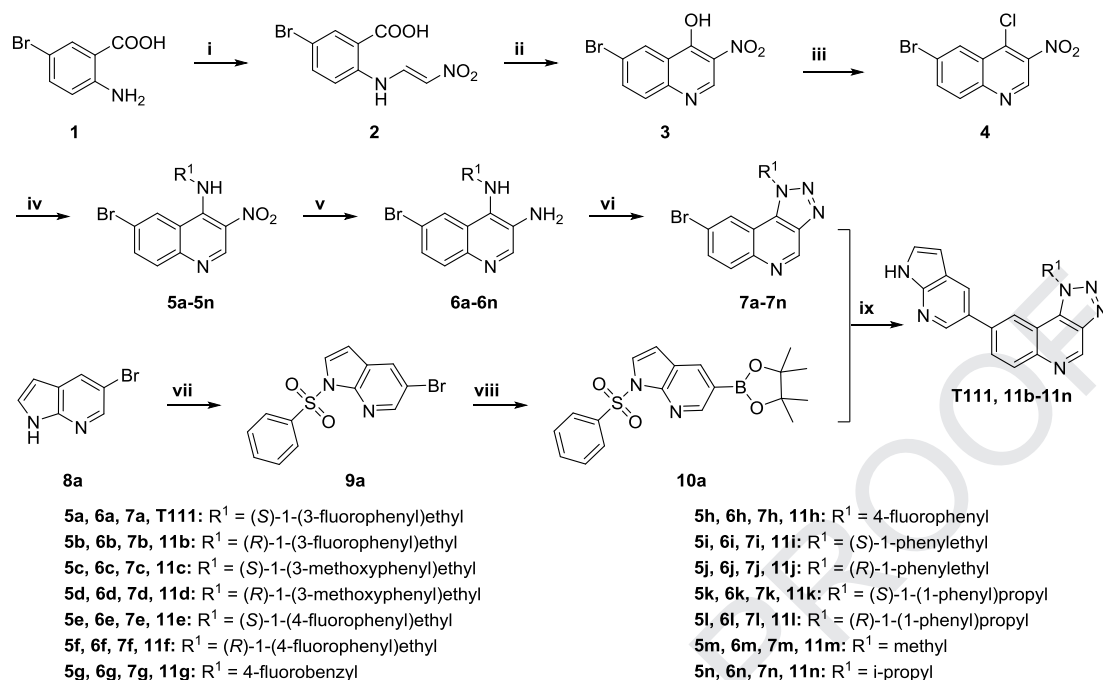


Figure 2. (A) Chemical structure of **T111**. (B) Focuses of the structural modification.

In the first step, we changed the R¹ group with different substituents and fixed R² as the original 1*H*-pyrrolo[2,3-*b*]pyridin-5-yl group. 15 compounds (**11b-n**) were synthesized. The synthetic routes for these compounds are depicted in Scheme 1. Briefly, commercially available 2-amino-5-bromobenzoic acid (**1**) reacted with 2-nitroacetaldehyde oxime to produce **2**, which was dehydrated to give **3**. Intermediate **4** was prepared through chlorination of **3**. Various amines then reacted with **4** to deliver **5a-5n** by nucleophilic substitution reactions, which were reduced to offer the corresponding amines **6a-6n**. **6a-6n** went through a diazotization and condensation to produce the triazoloquinoline compounds **7a-7n**. 7-Azaindole **8a** reacted with benzenesulfonyl chloride to give N-protected intermediate **9a**, which underwent Miyaura borylation to prepare **10a**. Compounds **T111** and **11b-n** were finally obtained through Suzuki coupling between **7a-7n** and **10a**, and subsequent deprotection by NaOH.

Scheme 1. Synthetic routes for compounds **11b-11n**, and **T111**.

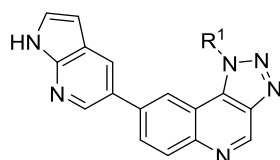


Reagents and conditions: (i) (1) HCl, H₂O, room temperature, (2) NaOH, H₂O, 0 °C, (3) HCl, H₂O, 0 °C; (ii) AcOK, Ac₂O, 120 °C; (iii) POCl₃, reflux; (iv) substituted amine, triethylamine, EtOH, reflux; (v) Fe, AcOH, 60 °C; (vi) NaNO₂, AcOH/H₂O; (vii) benzenesulfonyl chloride, NaH, THF, 0 °C; (viii) bis(pinacolato)diboron, PdCl₂(dppf), AcOK, 1,4-dioxane, 100 °C; (ix) (1) PdCl₂(dppf), K₂CO₃, 1,4-dioxane/H₂O, 100 °C; (2) NaOH, EtOH/H₂O, reflux.

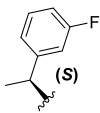
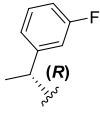
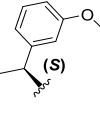
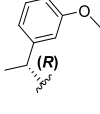
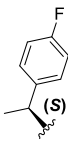
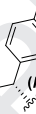
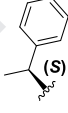
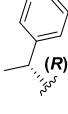
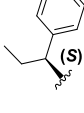
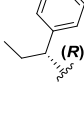
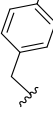
These compounds were then tested for their bioactivity on the A549-CTGF cell model at a series of concentrations (Table 1 and S1). Because **T111** contains an *S* configuration meta-fluoro-substituted 1-arylethyl group at the R¹ position, we first examined the bioactivity of enantiomer **11b** with an *R* configuration meta-fluoro-substituted 1-arylethyl group at the R¹ position. The result showed that the bioactivity of **11b** was obviously reduced compared with that of **T111**, indicating that the *S* configuration meta-fluoro-substituted 1-arylethyl group is more favorable than the

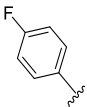

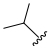
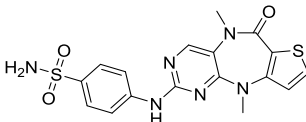
corresponding *R* configuration at the R^1 position. Replacement of the meta-fluoro with meta-methoxyl led to a decreased activity (**11c**). When the fluorine atom was moved to the para-position from meta-position on the phenyl group, the bioactivity improved remarkably (**11e** vs **T111**). We then tested the bioactivity of the unsubstituted compound **11g**, which gave a further enhanced potency. **11d**, **11f** and **11h** displayed weaker bioactivity than their corresponding enantiomer **11c**, **11e** and **11g**, which confirmed that the *S* configuration 1-arylethyl groups are preferred than the corresponding *R* configuration moieties at the R^1 position. Next, 1-phenylethyl group was changed to 1-phenylpropyl group, and the resulted compound **11i** exhibited reduced activity (**11i** vs **11g**). Again, *R* configuration 1-phenylpropyl compound **11j** displayed weaker potency compared with *S* configuration **11i**. Finally, we replaced the 1-arylethyl group with smaller substitution groups, including 4-fluoro-benzyl (**11k**), 4-fluoro-phenyl (**11l**), methyl (**11m**) and isopropyl (**11n**). Bioactivities of all the generated compounds significantly reduced. In short, the most potent compound obtained in this step corresponds to **11g**, which contains a (*S*)-1-phenylethyl group at the R^1 position.

Table 1 Bioactivities of compounds 11b-11n and T111^a



Compound	R^1	Relative level of firefly luciferase at 10 μ M
----------	-------	---

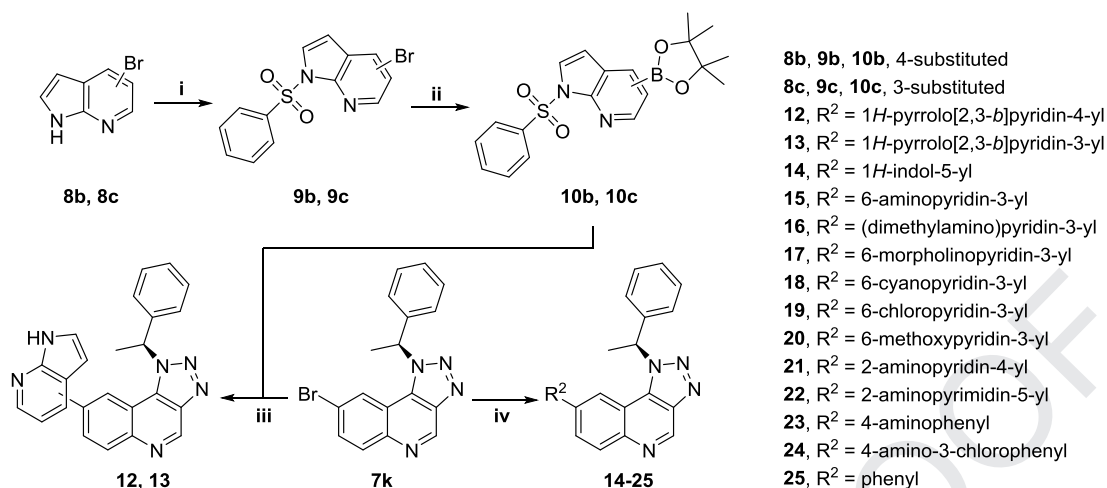
T111		4.909 ± 0.314
11b		2.096 ± 0.205
11c		3.131 ± 0.103
11d		2.224 ± 0.325
11e		6.509 ± 1.280
11f		4.922 ± 0.617
11g		13.540 ± 0.651
11h		8.099 ± 0.207
11i		8.059 ± 0.640
11j		3.717 ± 0.109
11k		3.872 ± 0.124

11l		3.443 ± 0.132
11m		0.550 ± 0.013
11n		3.382 ± 1.273
XMU-MP-1		4.923 ± 0.322

^a All assays were conducted in triplicate.

In the second step, we fixed R¹ as the optimal (*S*)-1-phenylethyl group and altered R² with various substituents. 14 new compounds (**12-25**) were synthesized. Reaction routes for these compounds are shown in Scheme 2. Briefly, through similar reaction routes as those for **10a** in Scheme 1, intermediates **10b** and **10c** were readily prepared. Target compounds **12** and **13** were obtained by Suzuki coupling of intermediate **7k** with **10b** and **10c** and then deprotection, respectively. Suzuki coupling reactions were conducted again between **7k** and various commercially available aromatic boric acid (or ester) to produce final products **14-25**.

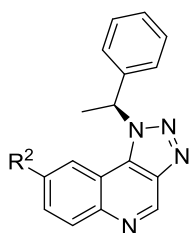
Scheme 2. Synthetic routes for compounds **12-25**.



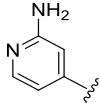
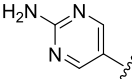
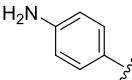
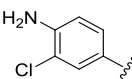
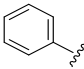
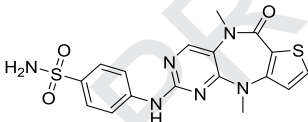
Reagents and conditions: (i) commercially available aromatic boric acid (or ester), benzenesulfonyl chloride, NaH, THF, 0 °C; (ii) bis(pinacolato)diboron, PdCl₂(dppf), AcOK, 1,4-dioxane, 100 °C; (iii) (1) PdCl₂(dppf), K₂CO₃, 1,4-dioxane/H₂O, 100 °C; (2) NaOH, EtOH/H₂O, reflux. (iv) PdCl₂(dppf), K₂CO₃, 1,4-dioxane/H₂O, 100 °C

Table 2 shows the bioactivities of compounds **12-25**. From Table 2, we can see that the change of linking position of 1*H*-pyrrolo[2,3-*b*]pyridyl group with the scaffold [1,2,3]triazolo[4,5-*c*]quinoline led to significantly decreased bioactivity (**12**, **13** vs **11g**). Replacement of the 1*H*-pyrrolo[2,3-*b*]pyridin-5-yl group with 5-indolyl also resulted in decreased bioactivity (**14**). We then replaced the R² position with various monocyclic groups, including substituted pyridyl (**15-21**), pyrimidyl (**22**) and phenyl (**23-25**). All the resulted compounds except **15** showed significantly decreased bioactivity or no activity; **15** showed a high bioactivity but still did not exceed **11g** in terms of the potency.

Table 2 Bioactivities of compounds 12-25^a



Compound	R ¹	Relative level of firefly luciferase at 10 μ M
12		0.549 \pm 0.0347
13		1.111 \pm 0.144
14		4.598 \pm 0.124
15		9.087 \pm 1.300
16		1.187 \pm 0.111
17		1.060 \pm 0.101
18		1.939 \pm 0.167
19		1.238 \pm 0.071
20		0.996 \pm 0.0154

21		2.012±0.253
22		3.486±0.510
23		2.242±0.090
24		1.728±0.066
25		1.428±0.092
XMU-MP-1		4.923±0.322

^a All assays were conducted in triplicate.

Overall, through the above structural optimization and SAR studies, we obtained a number of new Hippo signaling pathway inhibitors containing the scaffold [1,2,3]triazolo[4,5-*c*]quinoline. Among them, **11g** is the most potent one. Further bioactivity evaluation and mechanism studies were then carried out on this compound.

Firstly, we tested the effect of different concentrations of **11g** on the Hippo signaling pathway with the A549-CTGF cells. The results showed that **11g** dose-dependently increased the relative level of firefly luciferase (Figure 3A). Real-time PCR assays were then adopted to examine the influence of **11g** on the expression of target genes CTGF and cysteine rich angiogenic inducer 61 (Cyr61) of the Hippo signaling pathway.²⁰ As shown in Figure 3B and 3C, the mRNA levels of CTGF and

Cyr61 genes were up-regulated in a dose-dependent manner. Immunofluorescence assays were also used to test the impact of **11g** on the location of the effector protein YAP. The results showed that **11g** (10 μ M) led to nuclear translocation of YAP in A549-CTGF cells (Figure 3D). The positive control **XMU-MP-1** also showed the same effect but relatively weaker.

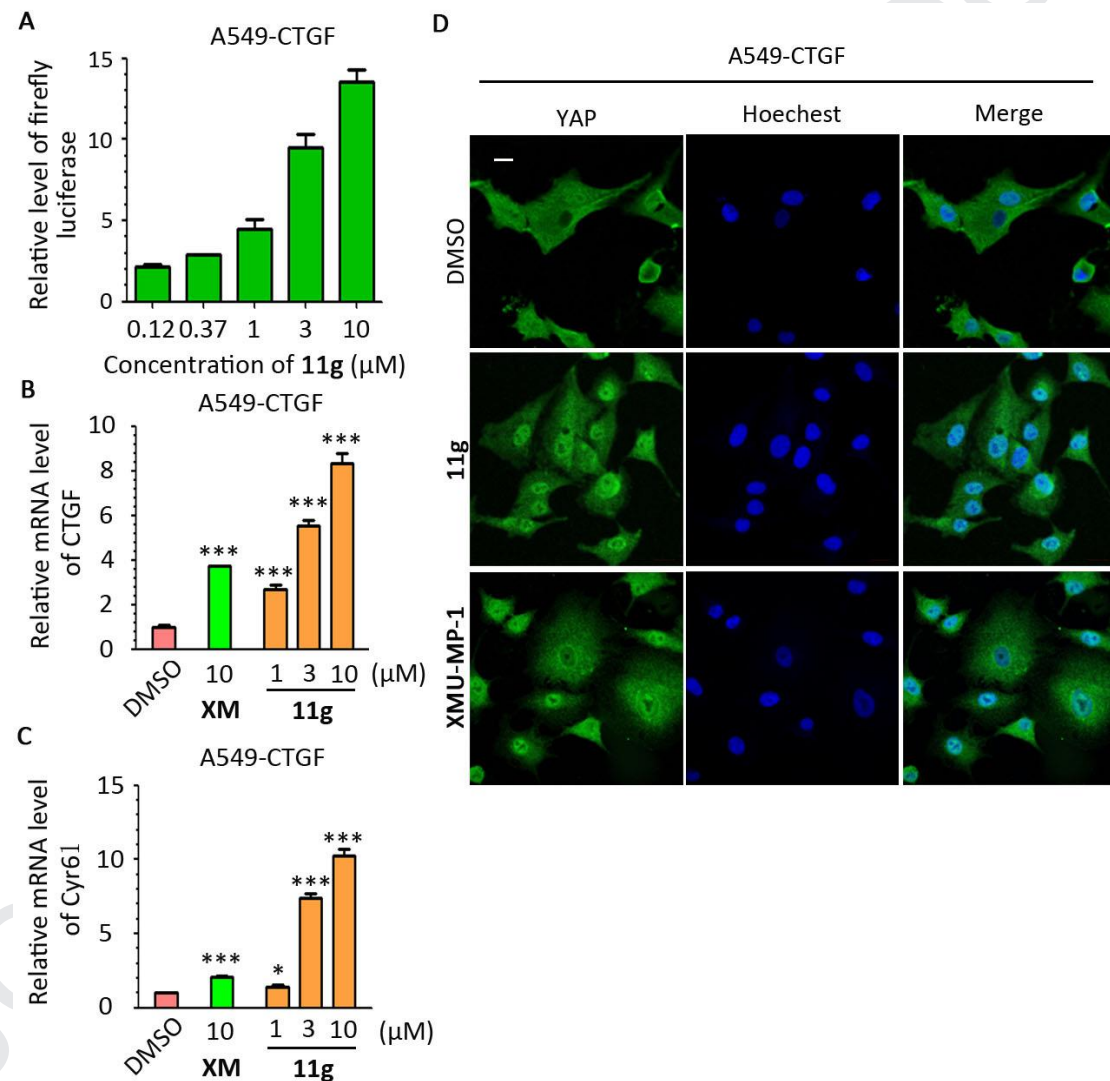


Figure 3. (A) **11g** dose-dependently increased relative firefly luciferase level in A549-CTGF cells. After treatment with **11g** for 24 h, A549-CTGF cells were subjected to dual-luciferase reporter assays. Data are represented as mean \pm SEM of three

independent experiments. The relative firefly luciferase level of DMSO-treated A549-CTGF cells was arbitrarily taken as 1. (B-C) **11g** significantly increased mRNA levels of endogenous CTGF (B) and Cyr61 (C) in A549-CTGF cells. A549-CTGF cells were treated with **11g**, **XMU-MP-1** (**XM**, 10 μ M) or DMSO (0.1%) for 24 h, and total RNA was extracted. The mRNA levels of endogenous CTGF and Cyr61 of A549-CTGF cells were detected by real-time PCR. Data (mean \pm SEM, n=4) were analyzed by Student's t-test. ***: $P < 0.001$; **: $P < 0.01$; *: $P < 0.05$. (D) **11g** promoted YAP nuclear translocation in A549-CTGF cells. A549-CTGF cells were fixed, penetrated, incubated with YAP antibodies and DAPI after treatment with **11g** (10 μ M), **XMU-MP-1** (10 μ M) or DMSO (0.1%) for 8 h. YAP antibodies were used to probe YAP, and DAPI was applied for nuclear staining. Scale bar: 10 μ m.

Then, a preliminary mechanism study was carried out on **11g**. To this end, we first tested the bioactivity of **11g** against the kinases MST1/2 through kinase profiling services provided by Eurofins. Unexpectedly, **11g** did not show activity against these kinases (Figure 4A). We then transferred to test the kinases LATS by KINOMEscan provided by DiscoverX (the Eurofins kinase profiling services do not include the kinases LATS). Again, **11g** did not display activity in this assay (Figure 4B). Here we can conclude that **11g** inhibits the Hippo signaling pathway through a mechanism different from that of **XMU-MP-1**, whose targets are MST1/2. To speculate potential targets of **11g**, we tested the inhibitory activity of **11g** against the other kinases (422 kinases) in the whole kinase panel of Eurofins through kinase profiling service (Table S2). In these assays, **11g** showed activity against about 118 kinases (an inhibitory rate > 50% at 10 μ M). Determining kinases whose inhibitions are responsible for the Hippo

pathway suppression needs a lot of work to do, which is still underway in our group and will be reported in near future.

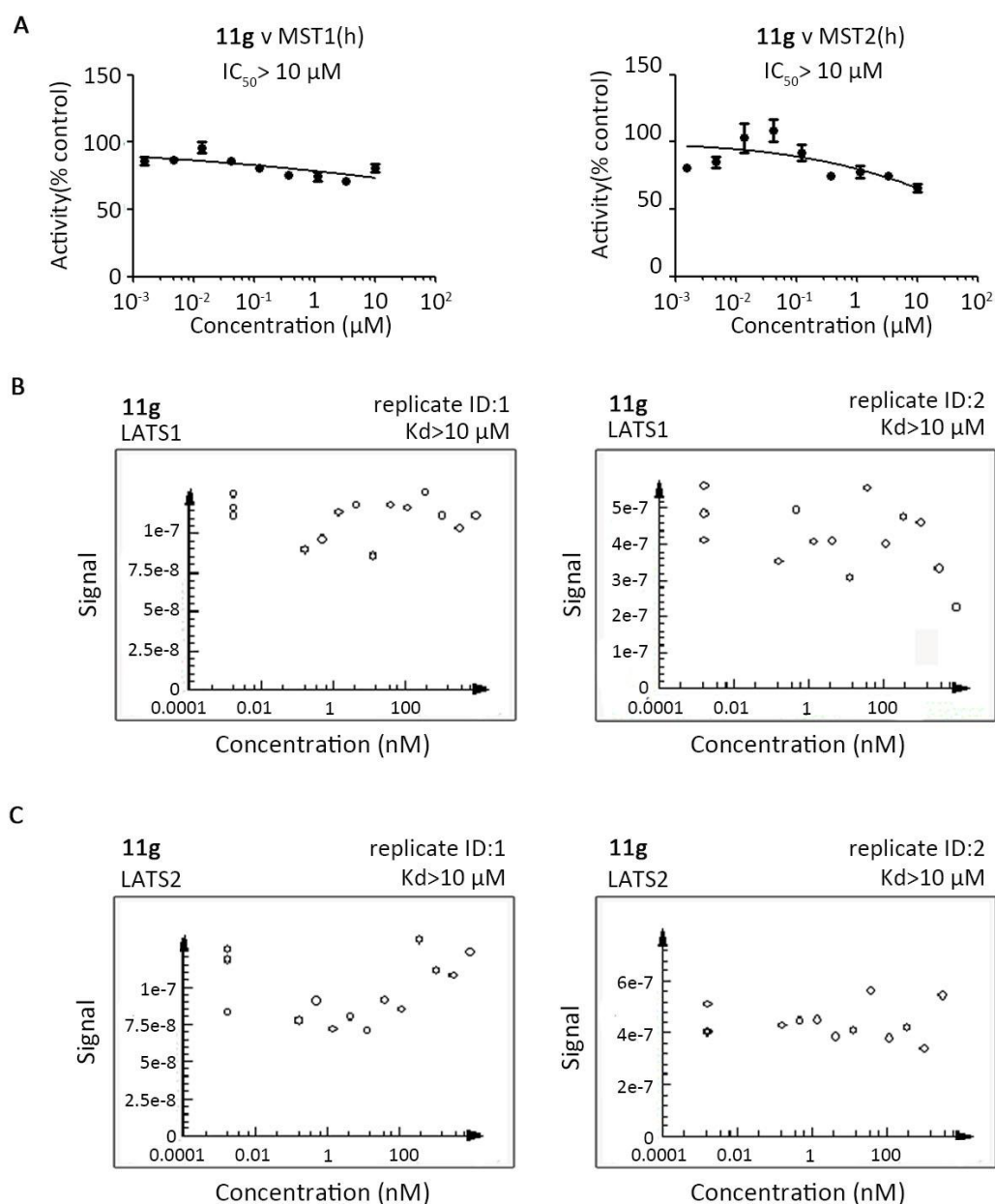


Figure 4. (A) **11g** showed no inhibitory activity against MST1 and MST2 in kinase profiling services provided by Eurofins. The data are the mean \pm SEM of 2 replicates. (B) Kd values of **11g** on LATS1/2 were greater than $10 \mu\text{M}$ in the KINOMEScan assay

provided by DiscoverX. The amount of kinase measured by qPCR (Signal; y-axis) is plotted against the corresponding concentration of **11g** in log10 scale (x-axis).

In summary, we in this investigation obtained a new potent Hippo pathway inhibitor (**11g**) by utilizing a cell line-based phenotype screening strategy and SAR analyses. This compound showed higher potency than **XMU-MP-1** in the CTGF dual-luciferase reporter system, real-time PCR and immunofluorescence assays *in vitro*. Nevertheless, the detailed targets of **11g** and mechanism of action are still unknown, which need further investigation.

ACKNOWLEDGEMENTS

This work was supported by the National Natural Science Foundation of China (81573349, 81773633, and 21772130), National Science and Technology Major Project (2018ZX09711002-014-002, 2018ZX09711002-011-019, 2018ZX09201018, and 2018ZX09711003-003-006), and 1.3.5 project for disciplines of excellence, West China Hospital, Sichuan University.

CONFLICTS OF INTEREST

The authors declare no conflicts of interest.

Supporting Information:

Supplementary data associated with this article can be found in the online version.

REFERENCES

1. Fan F, He Z, Kong LL, et al. Pharmacological targeting of kinases MST1 and MST2 augments tissue repair and regeneration. *Sci Transl Med*. 2016;8(352):352ra108. doi:10.1126/scitranslmed.aaf2304
2. Johnson R, Halder G. The two faces of Hippo: Targeting the Hippo pathway for regenerative medicine and cancer treatment. *Nat Rev Drug Discov*. 2014;13(1):63-79. doi:10.1038/nrd4161
3. Moya IM, Halder G. Hippo-YAP/TAZ signalling in organ regeneration and regenerative medicine. *Nat Rev Mol Cell Biol*. 2019;22:211-226. doi:10.1038/s41580-018-0086-y
4. Leach JP, Heallen T, Zhang M, et al. Hippo pathway deficiency reverses systolic heart failure after infarction. *Nature*. 2017;550(7675):260-264. doi:10.1038/nature24045
5. Piccolo S, Cordenonsi M, Dupont S. Molecular pathways: YAP and TAZ take center stage in organ growth and tumorigenesis. *Clin Cancer Res*. 2013;19(18):4925-4930. doi:10.1158/1078-0432.CCR-12-3172
6. Hong W, Guan KL. The YAP and TAZ transcription co-activators: Key downstream effectors of the mammalian Hippo pathway. *Semin Cell Dev Biol*. 2012;23(7):785-793. doi:10.1016/j.semcdb.2012.05.004
7. Harvey KF, Zhang X, Thomas DM. The Hippo pathway and human cancer. *Nat Rev Cancer*. 2013;13(4):246-257. doi:10.1038/nrc3458
8. Dupont S, Morsut L, Aragona M, et al. Role of YAP/TAZ in mechanotransduction. *Nature*. 2011;474(7350):179-184. doi:10.1038/nature10137
9. Zhao B, Wei X, Li W, et al. Inactivation of YAP oncoprotein by the Hippo pathway is involved in cell contact inhibition and tissue growth control. *Genes Dev*. 2007;21(21):2747-2761. doi:10.1101/gad.1602907.Hpo/Sav
10. Hao Y, Chun A, Cheung K, Rashidi B, Yang X. Tumor suppressor LATS1 is a negative regulator of oncogene YAP. *J Biol Chem*. 2008;283(9):5496-5509. doi:10.1074/jbc.M709037200
11. Totaro A, Panciera T, Piccolo S. YAP/TAZ upstream signals and downstream responses. *Nat Cell Biol*. 2018;20(8):888-899. doi:10.1038/s41556-018-0142-z
12. Zhang J, Ji J-Y, Yu M, et al. YAP-dependent induction of amphiregulin identifies a non-cell-autonomous component of the Hippo pathway. *Nat Cell Biol*. 2009;11:1444. doi:10.1038/ncb1993.
13. Johnson RL, Martin JF. Hippo Pathway Inhibits Wnt Signaling to Restrain Cardiomyocyte Proliferation and Heart Size. *Science*. 2011;6028(332):458-461. doi:10.1126/science.1199010
14. Grijalva JL, Huizenga M, Mueller K, et al. Dynamic alterations in Hippo signaling pathway and YAP activation during liver regeneration. *Am J Physiol Liver Physiol*. 2014;307(2):G196-G204. doi:10.1152/ajpgi.00077.2014
15. Lu L, Finegold MJ, Johnson RL. Hippo pathway coactivators Yap and Taz are required to coordinate mammalian liver regeneration. *Exp Mol Med*. 2018;50(1):e423. doi:10.1038/emmm.2017.205
16. Wang J, Liu S, Heallen T, Martin JF. The Hippo pathway in the heart: pivotal roles in development, disease, and regeneration. *Nat Rev Cardiol*. 2018;15(11):672-684. doi:10.1038/s41569-018-0063-3
17. Mani K, MBBS, Diwan A, MD. Drugging the Hippo (Pathway). *JACC Basic to Transl Sci*. 2018;3(5):654-656. doi:10.1016/j.jacbts.2018.09.003
18. Liu S, Martin JF. The regulation and function of the Hippo pathway in heart regeneration. *Wiley Interdiscip Rev Dev Biol*. 2019;8:e335. doi:10.1002/wdev.335

19. Liu Y, Yang F, Li J, et al. Mesenchymal stem cells enhance liver regeneration via improving lipid accumulation and Hippo signaling. *Stem Cells Int.* 2018;2018:1-11. doi:10.1155/2018/7652359
20. Lai D, Ho KC, Hao Y, Yang X. Taxol resistance in breast cancer cells is mediated by the hippo pathway component TAZ and its downstream transcriptional targets Cyr61 and CTGF. *Cancer Res.* 2011;71(7):2728-2738. doi:10.1158/0008-5472.CAN-10-2711